Tellus SERIES B CHEMICAL AND PHYSICAL METEOROLOGY
PUBLISHED BY THE INTERNATIONAL METEOROLOGICAL INSTITUTE IN STOCKHOLM

Tellus (2011), 63B, 196–204

TELLUS

Correlations between interannual variations of simulated global and regional CO_2 fluxes from terrestrial ecosystems and El Niño Southern Oscillation

By TAKAO IGUCHI*, *Disaster Prevention Research Institute, Kyoto University, Gokasho, Uji, 611-0011, Japan*

(Manuscript received 30 December 2009; in final form 14 September 2010)

ABSTRACT

Using a terrestrial ecosystem model (Sim-CYCLE), CO_2 exchange between the biosphere and the atmosphere was simulated for the period of 1980–2000. As a result, the biosphere was totally a sink of CO_2, and the phase of the interannual variation of the global annual CO_2 flux from the biosphere was similar to that of the annual increase of the global atmospheric CO_2. The interannual variation of the global annual CO_2 flux showed high correlation with that of the annual mean ENSO index (NINO.3 monitoring index) for a time lag of 1 yr. As for the regional annual carbon fluxes, some showed high correlation with the annual mean ENSO index for a time lag of 1 yr and some without time lag. Among the regional carbon fluxes those showed high correlations with ENSO index without time lag, some showed positive correlations and some showed negative correlations, and they canceled out each other in total. These negative correlations were found in tropical regions. All the regional carbon fluxes those showed high correlations with ENSO index for a time lag of 1 yr showed positive correlations.

1. Introduction

The atmospheric CO_2 keeps increasing year after year, but its annual growth rate has large interannual variation (Conway et al., 1994). The CO_2 emission from combustion of fossil fuel, the largest source of the atmospheric CO_2, is estimated to be quite constant with a small uncertainty (Marland et al., 2009). The estimation of the CO_2 emission from land use change has a large uncertainty (Houghton, 2003), though the interannual variation of the annual flux from this category is thought to be not as large as that of the annual increase of the atmospheric CO_2 because land use change is a human activity. Therefore, the absorption of the atmospheric CO_2 by terrestrial ecosystems and oceans seems to have a large interannual variation.

It is well known that there is a lagged correlation between the increase of the atmospheric CO_2 and ENSO index (Bacastow, 1976; Thompson et al., 1986; Elliott et al., 1991). Rayner et al. (1999) suggested that the correlation might be caused by initial response of the CO_2 fluxes from tropical oceans and later response of the terrestrial CO_2 fluxes to ENSO. However responses of terrestrial ecosystems to ENSO should not be globally simultaneous and uniform. It is very interesting why such a distinct lagged correlation is shown between ENSO and the global total carbon flux.

Interannual variations of terrestrial regional CO_2 fluxes were estimated by synthesis inversion methods using atmospheric transport models (Bousquet et al., 2000; Patra et al., 2005; Peylin et al., 2005; Gurney et al., 2008) and numerical simulations using terrestrial ecosystem models (Kindermann et al., 1996; Jones et al., 2001; Cao et al., 2005). Peylin et al. (2005) improved understanding of the interannual variation of the atmospheric CO_2 by comparing the results of an inversion method and model simulations. In most of the studies above, correlations between ENSO and anomalies of CO_2 fluxes were approached. Especially for the interannual variation of the anomaly of the carbon flux from tropical area, it is reported that its amplitude is dominant (Kindermann et al., 1996; Bousquet et al., 2000) and it tends to be positive in the year of El Niño (Bousquet et al., 2000; Jones et al., 2001; Patra et al., 2005). However the observed global total carbon flux to the atmosphere shows correlation with ENSO for a time lag of 1 yr. It is also an interesting point.

To investigate the contributions of the terrestrial regional carbon fluxes to the atmospheric CO_2, carbon exchange between the atmosphere and the biosphere was simulated using a

*Corresponding author.
e-mail: iguchi@dpac.dpri.kyoto-u.ac.jp
DOI: 10.1111/j.1600-0889.2010.00514.x

physiological process-based terrestrial ecosystem model (Sim-CYCLE). From the result, the interannual variation of the global annual carbon flux was compared with that of the annual increase of the atmospheric CO_2. Then, correlations between the global and regional annual carbon fluxes and the annual mean ENSO index were analysed, and contributions of the regional carbon fluxes to the global carbon flux were investigated.

2. Model and data

Sim-CYCLE (Simulation model of Carbon Cycle in Land Ecosystems) (Ito and Oikawa, 2002) calculates production by photosynthesis, distribution, respiration, litter fall and decomposition of organic matter on physiological processes. Sum of the emissions by respiration and decomposition minus the absorption by photosynthesis is treated as the carbon flux from the biosphere to the atmosphere. It is assumed that each grid area of the model is dominated by one of 11 vegetable types. In this version of the model, photosynthesis process does not depend on soil water. The horizontal resolution is 2.5 × 2.5 degree, and the time step is 1 d.

As external input data of Sim-CYCLE, downward shortwave radiation, total cloud cover, specific humidity, air temperature, pressure, soil moisture and soil temperature of NCEP/NCAR (National Centers for Environmental Prediction, National Oceanic and Atmospheric Administration/The National Center for Atmospheric Research, University Corporation for Atmospheric Research) Re-analysis data set and monthly CO_2 data of WMO/WDCGG (World Meteorological Organization/World Data Centre for Greenhouse Gases) were used. These data sets were spatially and temporary interpolated according to the grids and the time step of Sim-CYCLE.

3. Methods

To simulate the carbon exchange between the biosphere and the atmosphere, Sim-CYCLE was run for the period of 1751–2000. This section explains the details of the methods.

3.1. Change of atmospheric CO_2 for 1751–2000

This simulation needs atmospheric CO_2 data for the period of 1751–2000. To estimate the global mean atmospheric CO_2 concentration, ice core records (Neftel et al., 1985; Friedli et al., 1986; Siegenthaler et al., 1988; Barnola et al., 1995) were used. The global mean atmospheric CO_2 is assumed to be constant at 280 ppm until 1750. After 1959, it is assumed to be same as the annual mean data at Mauna Loa. For the period of 1751–1958, it is interpolated using the ice core records (Fig. 1). To obtain the horizontal distribution and its seasonal cycle of the CO_2 anomaly, WMO/WDCGG 1990 monthly data were interpolated spatially and temporarily. The anomaly distribution was added to the global annual mean CO_2 value of each year, and used as input data of Sim-CYCLE.

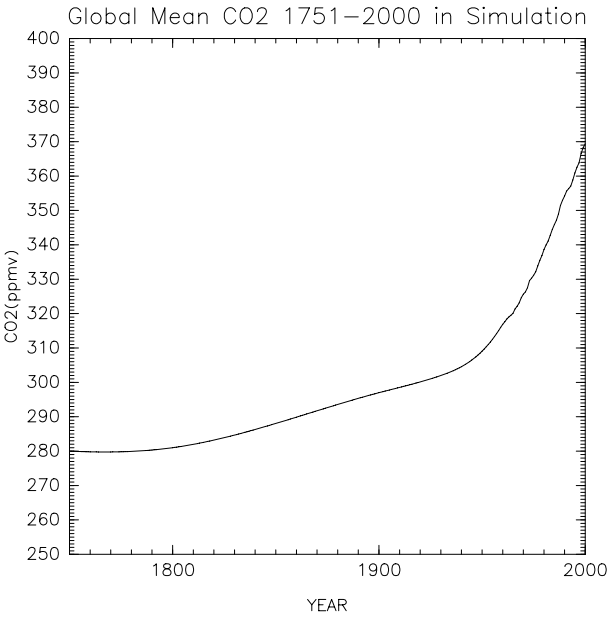

Fig. 1. Global annual mean atmospheric CO_2 for the period of 1751–2000 used in the simulation. Values for the period of 1959–2000 are annual means WMO/WDCGG monthly CO_2 data at Mauna Loa. Other values are interpolated using ice core record (Neftel et al., 1985; Friedli et al., 1986; Siegenthaler et al., 1988; Barnola et al., 1995).

3.2. Parameter adjustment and initial condition setting

Using 1951–2000 NCEP/NCAR Re-analysis climate data and 1990 WMO/WDCGG CO_2 data repeatedly, Sim-CYCLE was run until it reached a stable state. The model parameters were adjusted so as the plant and the soil carbon mass of all vegetation types in the stable state is within ±10% of the values of Whittaker and Likens (1975) and Post et al. (1982), respectively.

Then, using 1951–2000 NCEP/NCAR data and 1751 CO_2 data (obtained by the method of 3.1) repeatedly, Sim-CYCLE was run until it reached a stable state. The state is used as the initial condition of the simulation.

3.3. CO_2 increase experiment

From the initial condition obtained by the method of 3.2, Sim-CYCLE was run for the period of 1751–2000. Also in this experiment, 1951–2000 NCEP/NCAR Re-analysis data were used repeatedly.

4. Results

From the results of the simulation, correlations between the global and regional carbon fluxes and ENSO were verified for the period of 1980–2000. The land regions are same as TransCom 3

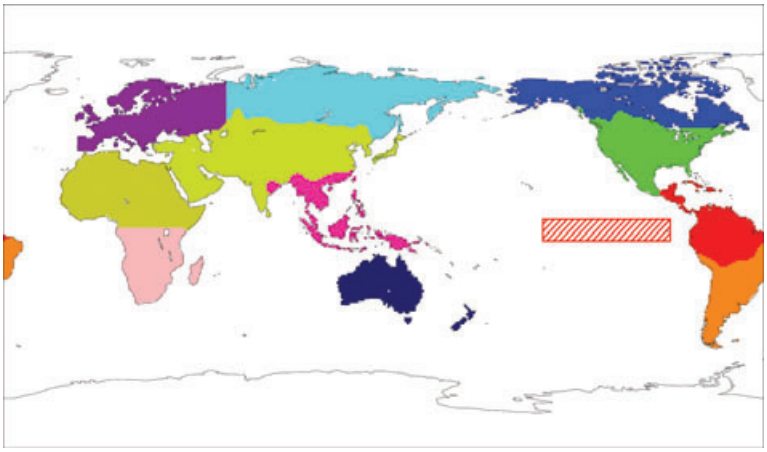

Fig. 2. Map of land regions and NINO.3 monitoring area (the red striped rectangle). The land regions are same as TransCom 3 experiment (Baker et al., 2006).

(Baker et al., 2006). As an index of ENSO, NINO.3 monitoring index of Japan Meteorological Agency (2009) was used. Figure 2 is a map of land regions and NINO.3 monitoring area.

4.1. *Correlation between the global annual carbon flux and ENSO*

As a result of the simulation, the total of terrestrial ecosystems was a carbon sink of 1.36 GtC yr^{-1} for the period of 1980–2000. The anomaly of the global annual carbon flux calculated by Sim-CYCLE from which its long-term trend was eliminated is shown in Fig. 3 (the solid line). Figure 3 also shows NOAA/ESRL (National Oceanic & Atmospheric Administration/Earth System Research Laboratory) annual increase data of the global atmospheric CO_2 (Tans and Conway, 2009) (the broken line) and the annual mean NINO.3 monitoring index (the dashed line). The interannual variation of the global carbon flux was comparable in phase to the variation of the atmospheric CO_2 increase, though its amplitude was about a half.

Next, correlation coefficients between the annual mean NINO.3 index and the global carbon flux or the atmospheric CO_2 increase were calculated. The correlation coefficients are calculated for time lags of 0 yr and 1 yr. The results are shown in Table 1. Both the global carbon flux and the atmospheric CO_2 increase showed higher correlations with ENSO for a time lag of 1 yr than 0 yr.

Figure 4 shows the interannual variations of the anomalies of the carbon fluxes from three latitudinal zones (90N–20N, 20N–20S and 20S–90S). The variation of the flux anomaly of tropical zone (20N–20S) was dominant in amplitude, and its phase was similar to the variation of the global carbon flux anomaly (Fig. 3).

4.2. *Correlations between the regional annual carbon fluxes and ENSO*

Figure 5 shows interannual variations of the regional and global annual carbon flux anomalies calculated by Sim-CYCLE (the

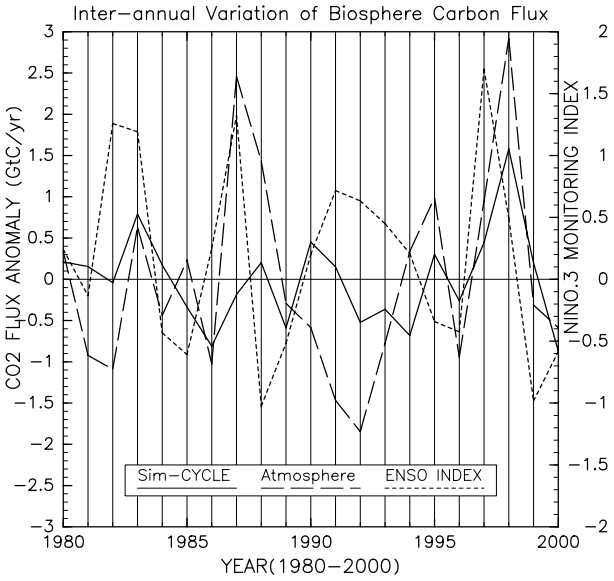

Fig. 3. Anomaly of the global annual carbon flux for the period of 1980–2000 simulated by Sim-CYCLE (the solid line). Long-term trend was eliminated. The broken line is the anomaly of NOAA/ESRL annual increase data of the atmospheric CO_2. Unit of the original NOAA/ESRL data is ppm, which was converted by the rate of 1 ppm = 2.1 GtC. Flux from the biosphere to the atmosphere is positive. The dashed line is the annual mean NINO.3 monitoring index of Japan Meteorological Agency.

black solid line). Figure 5 also shows the interannual variations of the anomalies of the regional and global mean NCEP/NCAR re-analysis data. The plotted parameters are air temperature (the red line), total cloud cover (the green line), specific humidity (the blue line) and soil moisture (the dark yellow line).

In the same way as the global carbon flux, correlation coefficients between the annual mean NINO.3 index and the regional annual fluxes were calculated. The results are shown in Table 2. In Table 2, Temperate North America, Tropical America, Temperate South America, Southern Africa and Tropical

Table 1. Correlation coefficients (r) between the annual mean NINO.3 monitoring index and the anomaly of the annual increase of the global atmospheric CO_2 or the global annual carbon flux simulated by Sim-CYCLE (shown in Fig. 3)

	0 yr lag	1 yr lag
Anomaly of the annual increase of the atmospheric CO_2	0.12	0.41
Anomaly of the global annual carbon flux of Sim-CYCLE	0.28	0.57

Note: Significant level is 95% for $|r| \geq 0.43$ and 90% for $|r| \geq 0.37$.

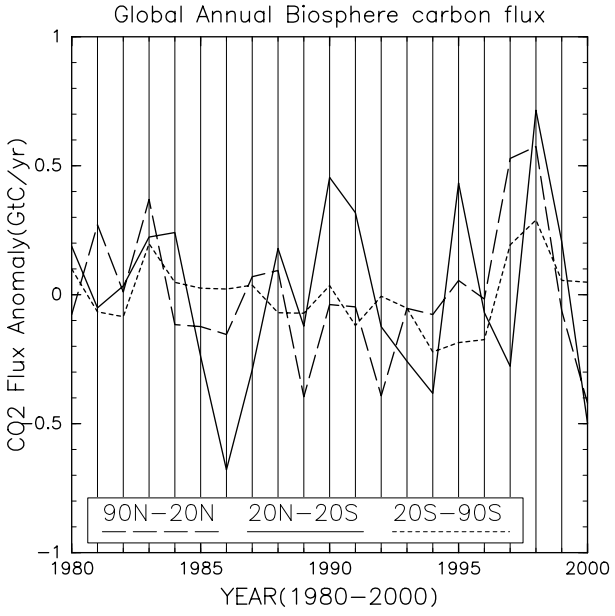

Fig. 4. Anomalies of annual carbon fluxes from three latitudinal belts for the period of 1980–2000 simulated by Sim-CYCLE. The three belts are 90N–20N (the broken line), 20N–20S (the solid line) and 20S–90S (the dashed line). Long-term trend was eliminated. Flux from the biosphere to the atmosphere is positive.

Asia showed higher correlations for a time lag of 0 yr than 1 yr. Northern Africa showed high correlation both for time lags of 0 yr and 1 yr. It is noticeable that Tropical America and Tropical Asia showed negative high correlations for a time lag of 0 yr. As for the regions where the correlation coefficients are larger for a time lag of 1 yr than 0 yr, only positive correlation coefficients were calculated.

To understand the difference of the regional responses, correlations between the regional and global annual mean NCEP/NCAR parameters and the regional and global carbon fluxes were analysed. The results are shown in Table 3. In most of the regions, the regional carbon flux showed high correlation with the total cloud cover (Table 3). For the air temperature, several regional fluxes showed low correlations, but the global carbon flux showed higher correlation with the global mean air temperature than with the global mean total cloud cover. The correlation between the regional carbon flux and the specific humidity was high in most of the regions, but the correlation coefficient was a positive value. Like the case of the total cloud cover, the regional carbon flux showed high correlation with the regional mean soil moisture in most of the regions, but the correlation between the global carbon flux and the global mean soil moisture was not high. Correlations between the annual mean NINO.3 index and the regional and global annual mean NCEP/NCAR parameters were also analysed. The results were shown in Table 4.

5. Discussion

The interannual variation of the global annual carbon flux anomaly calculated by Sim-CYCLE was similar to that of the annual increase of the atmospheric CO_2 in phase and showed high correlation with the annual mean NINO.3 monitoring index for a time lag of 1 yr (Fig. 3). These two variations are similar even in the first half of 1990s, in which the correlation between the increase of atmospheric CO_2 and the NINO.3 index is low. In this period, the interannual variation of the global annual carbon flux of Sim-CYCLE was very similar to that of the global annual mean NCEP/NCAR temperature data of land grids (Fig. 5). The global annual mean temperature declined for the period of 1992–1993 in spite of El Niño. It is suggested that this decline was due to the eruption of Mt. Pinatubo (Hansen et al., 1996). Considering that responses of the fluxes from the biosphere and oceans to ENSO cycle differ (Jones et al., 2001), the results of the simulation may suggest that the global flux from the biosphere play a primary role in the interannual variation of the atmospheric CO_2. However, as shown in Fig. 3, the amplitude of the interannual variation of the global annual flux calculated by Sim-CYCLE was much smaller than that of the annual increase of the atmospheric CO_2. To explain this difference, sensitivity of the model to climate change must be inspected. In addition, the fluxes from oceans, intensification of the flux from the biosphere by water stress in drought and the flux by fire must be taken into account.

As for the regional carbon fluxes, some regions showed high correlations with NINO.3 index without time lag (Table 2). By analysing the regional monthly flux and the monthly mean ENSO index, Jones et al. (2001) and Patra et al. (2005) showed that the early reaction starts within a few months. However, this study focuses on the contribution of the regional fluxes to the interannual variation of the increase of the global atmospheric CO_2, so the regional annual fluxes were analysed. In Table 2, it seems that the fluxes from the regions those are in tropical area or close to NINO.3 monitoring area tend to show high correlations with ENSO without time lag, though there are exceptions (e.g. Australia).

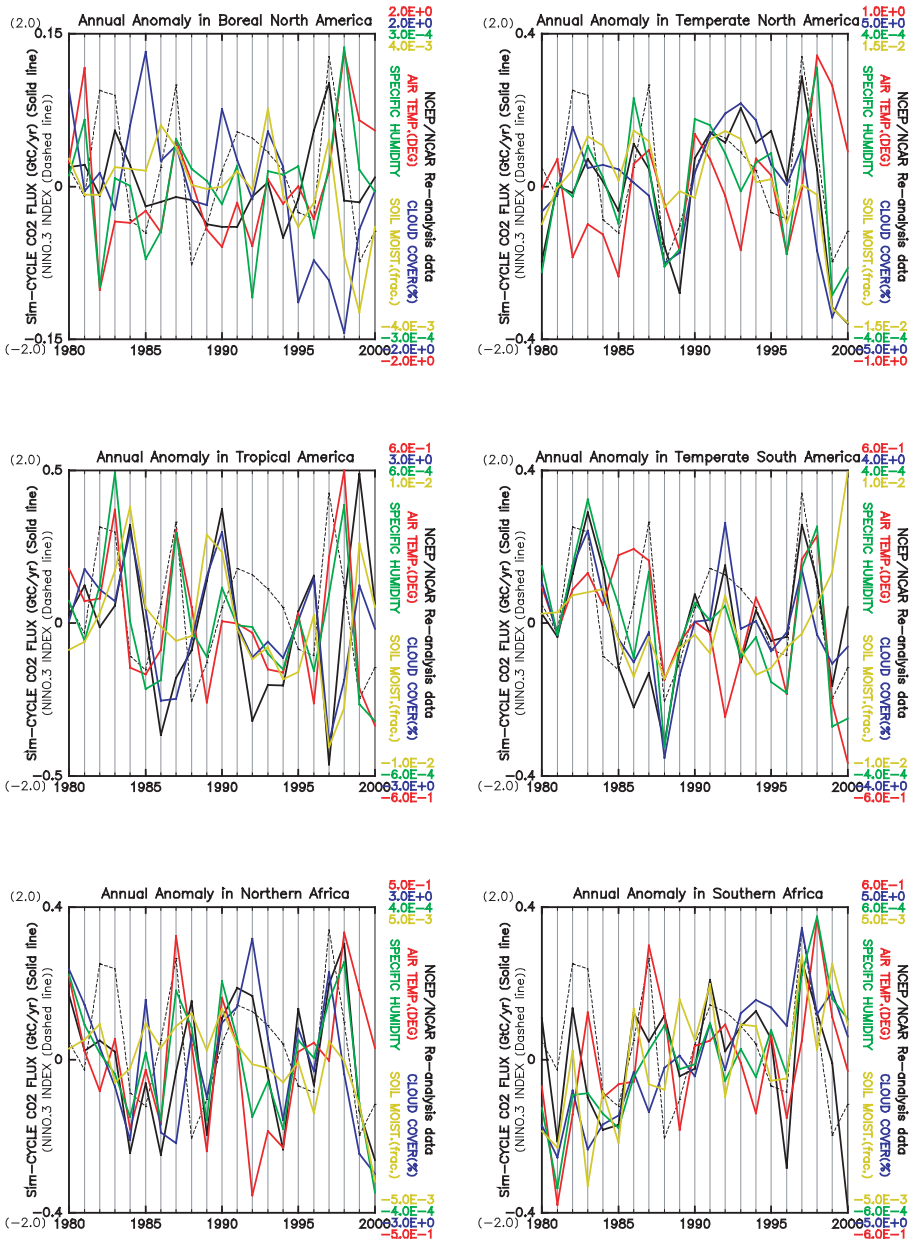

Fig. 5. Anomalies of regional and global annual carbon fluxes calculated by Sim-CYCLE (the black solid line). Long-term trend was eliminated. Flux from the biosphere to the atmosphere is positive. This figure also shows anomalies of annual mean air temperature (the red line), total cloud cover (the green line), specific humidity (the blue line) and soil moisture (the dark yellow line) of NCEP/NCAR Re-analysis data averaged for each region. The values of soil moisture are averages of 0–10 cm and 10–200 cm layers. The black dashed line is NINO.3 monitoring index.

Among the regional fluxes those have high correlations with NINO.3 index without time lag, fluxes from Tropical America and Tropical Asia showed negative high correlations. The correlation coefficient between the annual mean NINO.3 index and the global annual flux for a time lag of 0 yr is 0.28 (Table 1), however, without these two regions, the correlation coefficient rises to 0.61. This result suggests that the regional fluxes of negative correlations and other regional fluxes of positive correlations are cancelling out each other. As for the global flux without Tropical America and the global flux without Tropical Asia, correlation coefficients with NINO.3 index for a time lag of 0 yr are 0.48 and 0.39, respectively. Though the absolute value of the correlation coefficient of the flux from Tropical America is less than that of the flux from Tropical Asia (Table 2), it seems that the cancelling effect of the flux from Tropical America is greater than that of the flux from Tropical Asia.

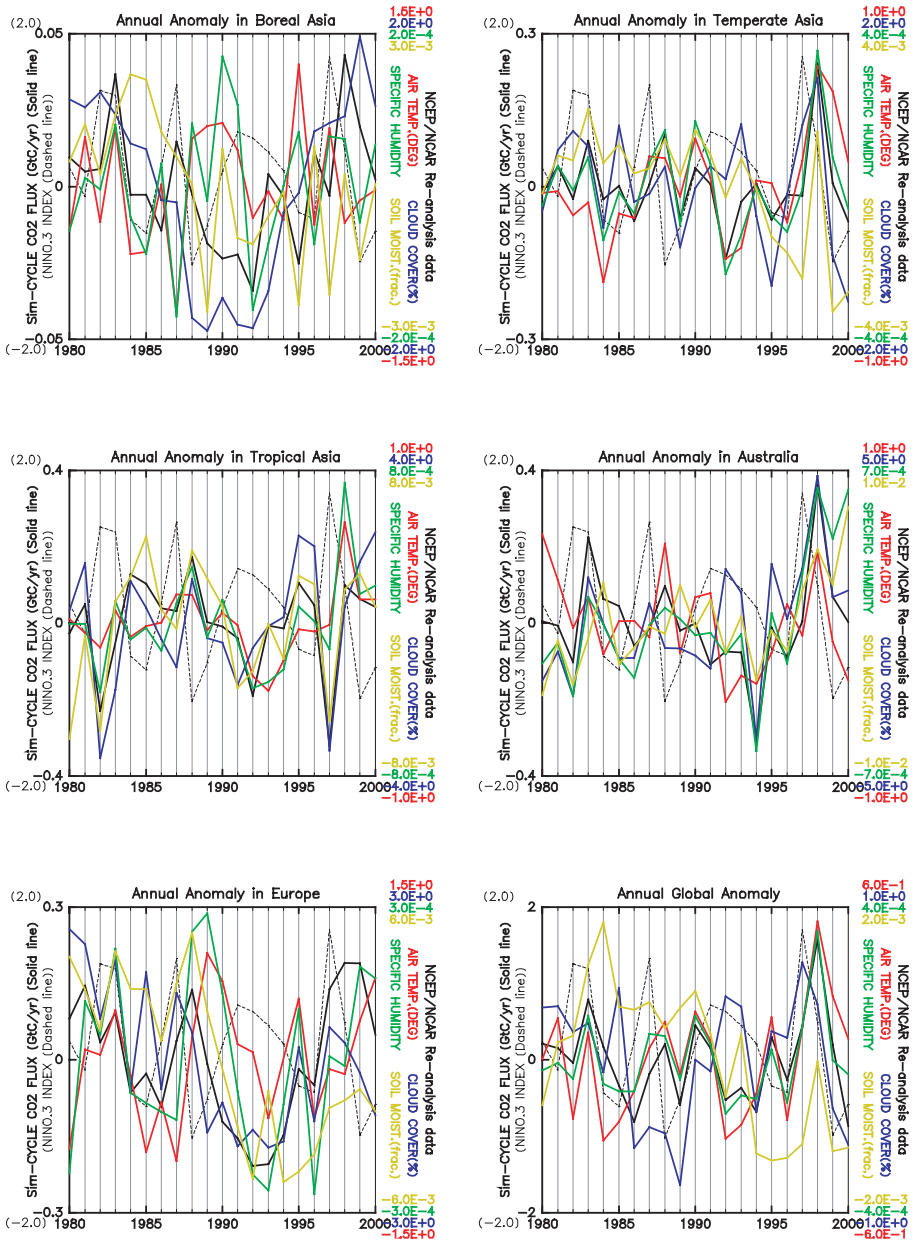

Fig. 5. Continued

Figure 4 shows that the amplitude of the flux anomaly from the tropical zone was dominant. This agrees with Kindermann et al. (1996) and Bousquet at al. (2000). However its phase is similar to the phase of the global total carbon flux and showed a high correlation for a time lag of 1 yr. If the interannual variation of the flux from the tropical zone has both dominant amplitude and positive correlation without time lag, the global total carbon flux will have a high correlation with ENSO without time lag. The observation of the atmospheric CO_2 increase that shows a high correlation with ENSO for a time lag of 1 yr suggests the existence of a cancelling effect of the regional fluxes from tropical area. Although the oceans play a role of cancelling (Feely et al., 1987; Rayner et al., 1999; Jones et al., 2001), Sim-CYCLE suggested the existence of another cancelling effect.

Table 3 shows that there are high correlations between the regional annual carbon fluxes and the total cloud cover. Especially in Tropical America and Tropical Asia, there are high negative correlations between NINO.3 index and the total cloud cover without time lag (Table 4), those are consistent with the high correlations between the total cloud cover and the regional fluxes. These negative correlations between ENSO and the

Table 2. Correlation coefficients (r) between the annual mean NINO.3 monitoring index and the regional annual carbon fluxes calculated by Sim-CYCLE (shown in Fig. 5)

Region	0 yr lag	1 yr lag
Boreal North America	0.29	−0.10
Temperate North America	0.61	0.12
Tropical America	−0.58	0.21
Temperate South America	0.66	−0.08
Northern Africa	0.24	0.45
Southern Africa	0.46	0.11
Boreal Asia	0.13	0.46
Temperate Asia	−0.07	0.66
Tropical Asia	−0.71	0.51
Australia	−0.06	0.61
Europe	−0.03	0.39

Note: Significant level is 95% for $|r| \geq 0.43$ and 90% for $|r| \geq 0.37$.

regional fluxes do not agree with Patra et al. (2005). The version of Sim-CYCLE of this study may be too sensitive to the solar radiation. In Temperate North America and Temperate South America, there are high positive correlations between NINO.3 index and the total cloud cover without time lag (Table 4), and high positive correlations between the total cloud cover and the regional fluxes (Table 3). In other regions, no correlation between ENSO and the total cloud cover or other parameters of NCEP/NCAR Re-analysis data that are clearly consistent with the correlation between NINO.3 and the regional carbon flux was found. It is interesting that these consistent correlations were found in the regions where the correlation coefficients between ENSO and the regional fluxes are higher for a time lag of 0 yr than 1 yr. The positive correlation coefficients between the specific humidity and the regional carbon fluxes (Table 3) are thought to be due to high correlations between the specific humidity and the total cloud cover and the air temperature, and superiority of the positive effect of the total cloud cover and the air temperature to the negative effect of the specific humidity.

6. Conclusions

As a result of the simulation using the terrestrial ecosystem model, the global annual carbon flux from the biosphere showed an interannual variation, which is similar to that of the annual increase of the global atmospheric CO_2 and a high correlation with ENSO for a time lag of 1 yr. This result suggests the domination of the flux from the biosphere in the interannual variation of the atmospheric CO_2 increase. As for the regional carbon fluxes, the fluxes from tropical regions those showed negative correlations with ENSO for a time lag of 0 yr cancelled out the fluxes those showed positive correlations for a time lag of 0 yr. In the regions where the regional carbon fluxes showed negative correlations with ENSO, there were also high correlations between ENSO and the total cloud cover and between the total cloud cover and the regional carbon fluxes. This result suggests the important contribution of solar radiation to the 1-yr-lagged correlation between ENSO and the global carbon flux from the biosphere.

7. Acknowledgments

The original Sim-CYCLE model was presented by Akihiko Ito (NIES) and independently modified for this study. NOAA/ESRL atmospheric CO_2 increase data, NCEP/NCAR Re-analysis climate data, Japan Meteorological Agency NINO.3 monitoring index data, and TransCom 3 land region map were downloaded

Table 3. Correlation coefficients (r) between the regional or global annual mean NCEP/NCAR Re-analysis data and regional or global annual carbon fluxes calculated by Sim-CYCLE (shown in Fig. 5)

Region	Air temperature	Total cloud cover	Specific humidity	Soil moisture
Boreal North America	0.12	−0.30	0.03	0.23
Temperate North America	−0.07	0.81	0.77	0.75
Tropical America	−0.21	0.84	−0.06	0.72
Temperate South America	0.20	0.85	0.71	0.41
Northern Africa	0.41	0.75	0.78	0.46
Southern Africa	0.37	0.39	0.41	0.40
Boreal Asia	−0.34	0.67	−0.06	0.36
Temperate Asia	0.63	0.54	0.91	0.45
Tropical Asia	0.38	0.79	0.56	0.79
Australia	0.50	0.70	0.73	0.44
Europe	0.08	0.66	0.52	0.43
Global	0.68	0.47	0.86	0.15

Note: Significant level is 95% for $|r| \geq 0.43$ and 90% for $|r| \geq 0.37$.

Table 4. Correlation coefficients (r) between the annual mean NINO.3 monitoring index and the regional or global annual mean NCEP/NCAR Re-analysis data (shown in Fig. 5)

Region	Air temperature		Total cloud cover		Specific humidity		Soil moisture	
	0 yr	1 yr	0 yr	1 yr	0 yr	1 yr	0 yr	1 yr
Boreal North America	−0.15	0.29	−0.07	−0.23	0.01	0.41	0.47	−0.14
Temperate North America	0.01	0.23	0.58	0.03	0.59	0.25	0.55	0.28
Tropical America	0.64	0.53	−0.49	−0.05	0.66	0.52	−0.45	−0.12
Temperate South America	0.52	0.14	0.69	0.10	0.72	0.29	−0.06	−0.05
Northern Africa	0.08	0.18	0.26	0.05	0.36	0.26	0.28	0.11
Southern Africa	0.28	0.47	0.03	−0.14	0.12	0.18	0.04	−0.37
Boreal Asia	−0.10	−0.14	0.02	0.03	0.00	−0.03	−0.06	0.19
Temperate Asia	−0.05	0.09	0.51	0.38	0.08	0.36	0.22	0.39
Tropical Asia	−0.09	0.22	−0.84	0.06	−0.28	0.34	−0.70	0.13
Australia	−0.03	0.31	0.13	0.37	−0.14	0.15	−0.19	−0.02
Europe	−0.24	−0.16	0.18	0.20	−0.28	−0.06	−0.06	0.16
Global	0.00	0.23	0.40	0.27	0.27	0.41	0.13	0.21

Note: Significant level is 95% for $|r| \geq 0.43$ and 90% for $|r| \geq 0.37$.

from their homepages. As for CO_2 observation data, use was made of WMO/WDCGG CD-ROM. The figures were produced by GFD-DENNOU Library.

References

Bacastow, R. B. 1976. Modulation of atmospheric carbon dioxide by the southern oscillation. *Nature* **261**, 116–118.

Baker, D. F., Law, R. M., Gurney, K. R., Rayner, P., Peylin, P. and co-authors. 2006. TransCom 3 inversion intercomparison: impact of transport model errors on the interannual variability of regional CO_2 fluxes, 1988–2003. *Global Biogeochem. Cycles* **20**, 1002, doi:10.1029/2004GB002439.

Barnola, J. M., Anklin, M., Porcheron, J., Raynaud, D., Schwander, J. and co-authors. 1995. CO_2 evolution during the last millennium as recorded by Antarctic and Greenland ice. *Tellus* **47B**, 264–272.

Bousquet P., Peylin, P., Ciais, P., Quéré, C. L., Friedlingstein, P. and co-authors. 2000. Regional changes in carbon dioxide fluxes of land and oceans since 1980. *Science* **290**, 1342–1346.

Cao, M., Prince, S. D., Tao, B., Small, J. and Li, K. 2005. Regional pattern and interannual variations in global terrestrial carbon uptake in response to changes in climate and atmospheric CO_2. *Tellus* **57B**, 210–227.

Conway, T. J., Tans, P. P., Waterman, L. S., Thoning, K. W., Kitzis, D. R. and co-authors. 1994. Evidence for interannual variability of the carbon cycle from the National Oceanic and Atmospheric Administration/Climate Monitoring and Diagnostics Laboratory Global Air Sampling Network. *J. geophys. Res.* **99**, 22831–22855.

Elliott, W. P., Angell, J. K. and Thoning, K. W. 1991. Relation of atmospheric CO_2 to tropical sea and air temperature and precipitation. *Tellus* **43B**, 144–155.

Feely, R. A., Gammon, R. H., Taft, B. A., Pullen, P. E., Waterman, L. S. and co-authors. 1987. Distribution of chemical tracers in the Eastern Equatorial Pacific during and after the 1982–83 El Niño/Southern Oscillation event. *J. geophys. Res.* **92**, 6545–6558.

Friedli, H., Loetscher, H., Oeschger, H., Siegenthaler, U. and Stauffer, B. 1986. Ice core record of the $^{13}C/^{12}C$ ratio of atmospheric CO_2 in the past two centuries. *Nature* **324**, 237–238.

Gurney, K. R., Baker, D., Rayner, P. and Denning, S. 2008. Interannual variations in continental-scale net carbon exchange and sensitivity to observing networks estimated from atmospheric CO_2 inversions for the period 1980 to 2005. *Global Biogeochem. Cycles* **22**, 3025, doi:10.1029/2007GB003082.

Hansen, J., Ruedy, R., Sato, M. and Reynolds R. 1996. Global surface temperature in 1995: return to pre-Pinatubo level. *Geophys. Res. Lett.* **23**, 1665–1668.

Houghton, R. A. 2003. Revised estimates of the annual net flux of carbon to the atmosphere from changes in land use and land management 1850–2000. *Tellus* **55B**, 378–390.

Ito A. and Oikawa, T. 2002. A simulation model of the carbon cycle in land ecosystems (Sim-CYCLE): a description based on dry-matter production theory and plot-scale validation. *Ecol. Model.* **151**, 143–176.

Japan Meteorological Agency. 2009. 'El Nino monitoring and outlook'. Available at: ds.data.jma.go.jp/tcc/tcc/products/elnino. Last accessed 30 Dec 2009.

Jones, C. D., Collins, M., Cox, P. M. and Spall S. A. 2001. The carbon cycle response to ENSO: a coupled climate-carbon cycle model study. *J. Clim.* **14**, 4113–4129.

Kindermann, J., Würth, G., Kohlmaier, G. H. and Badeck, F. W. 1996. Interannual variation of carbon exchange fluxes in terrestrial ecosystems. *Global Biogeochem. Cycles.* **10**, 737–355.

Marland, G., Boden, T. A. and Andres, R. J. 2009. *Global, Regional, and National Fossil Fuel CO_2 Emissions, in Trends: A Compendium of Data on Global Change*. Carbon Dioxide Information Analysis Center, Oak Ridge National Laboratory, U.S. Department of Energy, Oak Ridge, Tenn.

Neftel, A., Moor, E., Oeschger, H. and Stauffer, B. 1985. Evidence from polar ice cores for the increase in atmospheric CO_2 in the past two centuries. *Nature* **315**, 45–57.

Patra, P. K., Ishizawa, M., Maksyutov, S., Nakazawa, T. and Inoue, G. 2005. Role of biomass burning and climate anoalies for

land-atmosphere carbon fluxes based on inverse modeling of atmospheric CO_2. *Global Biogeochem. Cycles.* **19**, 3005, doi:10.1029/2004GB002258.

Peylin, P., Bousquet, P., Quéré, C. L., Sitch, S., Friedlingstein, P. and co-authors. 2005. Multiple constraints on regional CO_2 flux variations over land and oceans. *Global Biogeochem. Cycles* **19**, 1011, doi:10.1029/2003GB002214.

Post, W. M., Emannuel, W. R., Zinke, P. Z. and Stangenberger, A. G. 1982. Soil carbon pools and world life zones. *Nature* **298**, 156–159.

Rayner, P. J., Law, R. M. and Dargaville, R. 1999. The relationship between tropical CO_2 fluxes and the El Niño-Southern oscillation. *Geophys. Res. Lett.* **26**, 493–496.

Siegenthaler, U., Friedli, H., Loeeetscher, H., Moor, E., Neftel, A. and co-authors. 1988. Stable-isotope ratios and concentration of CO_2 in air from polar ice cores. *Ann. Glaciol.* **10**, 151–156.

Tans, P. P. and Conway, T. J. 2009. 'Globally averaged marine surface annual mean growth rates. NOAA/ESRL'. Available at: www.esrl.noaa.gov/gmd/ccgg/trends. Last accessed 30 Dec 2009.

Thompson, M. L., Enting, I. G. Pearman, G. I. and Hyson, P. 1986. Interannual variation of atmospheric CO_2 concentration. *J. Atmos. Chem.* **4**, 125–155.

Whittaker, R. H. and Likens, G. E. 1975. The biosphere and man. *The Primary Productivity of the Biosphere*. Springer Verlag, New York, 305–328.